

Metabolomic profiling of female mink serum during early to mid-pregnancy to understand factors associated with embryo diapause

zheng li

Jilin University

chengjun liu

Jilin University

liang deng

Jilin University

maosheng cao

Jilin University

xue zheng

Jilin University

lu chen

Jilin University

chenfeng yuan

Jilin University

zijiao zhao

Jilin University

chunjin li (✉ llcjj158@163.com)

Research

Keywords: Metabolomic profiling, embryo diapause, Mink, Reactivation, Amino 12 acid, Dopamine

Posted Date: May 6th, 2020

DOI: <https://doi.org/10.21203/rs.3.rs-23706/v1>

License: © ⓘ This work is licensed under a Creative Commons Attribution 4.0 International License.

[Read Full License](#)

1 **Metabolomic profiling of female mink serum during early to**
2 **mid-pregnancy to understand factors associated with**
3 **embryo diapause**

4 **Zheng Li¹, Chengjun Liu¹, Liang Deng¹, Maosheng Cao¹, Xue Zheng¹, Lu**
5 **Chen¹, Chenfeng Yuan¹, Zijiao Zhao¹, Chunjin Li^{2*}**

6 ¹ College of Animal Sciences, Jilin University, Changchun, China.

7 ² College of Animal Sciences, Jilin University, Changchun, China

8 *** Correspondence:**

9 Professor Chunjin Li
10 llcjj158@163.com

11 **Keywords:** Metabolomic profiling; Embryo diapause; Mink; Reactivation; Amino
12 acid; Dopamine

13 **Highlights:**

14 We examined changes in the chemical composition of the serum extracts taken during
15 the different stages of pregnancy.

16 Dopamine may be the major inhibitory compound for mink embryo reactivation

17 The levels of L-proline, L-threonine, taurine, D-ornithine, L-valine, L-kynurenine,
18 and particularly L-leucine may be related to embryo reactivation.

19 **Abstract**

20 **Background :** The mink exhibits embryo diapause after fertilization. Mink embryos
21 enter a period of diapause after the embryo develops into the blastocyst. The specific
22 process of embryo diapause regulation and reactivation is remains largely
23 un-examined. The aim of this study was to identify key factors associated with mink
24 embryo diapause and reactivation by comparing and analyzing differences in serum
25 metabolites up to twenty-nine days after mating.

26 **Material and methods:** Blood samples were taken on the first day of mating, and then
27 once a week until the fifth week. Metabolomic profiles of the serum samples taken
28 during this period were analysed by ultra-performance liquid chromatography/mass
29 spectrometry.

30 Results: Multivariate statistical analyses identified differential metabolite expression
31 at different time points in both positive ion mode and negative ion modes. Dopamine
32 may be the major inhibitory compound for mink embryo reactivation; moreover, and
33 the levels of L-proline, L-threonine, taurine, D-ornithine, L-valine, L-kynurenine, and
34 particularly L-leucine may be related to embryo reactivation.

35 Conclusions: We compared blood serum metabolites at different stages in the
36 pregnancy. The study makes a significant contribution to the literature as we found
37 that dopamine is a strong candidate as an inhibitor of embryo reactivation. The study
38 showed that levels of seven amino acids, but especially L-leucine, may be correlated
39 with embryo reactivation.

40 **1 Introduction**

41 The American mink (*Neovison vison*) exhibits seasonal estrus and
42 mating-stimulated ovulation. When the fertilized oocyte develops into a blastocyst,
43 the embryo is discharged from the uterus and enters a relatively static developmental
44 state, called embryo diapause[1]. Birth of the offspring is postponed by delayed
45 implantation of blastocysts so that offspring are born during favorable environmental
46 conditions of temperature and food availability. This reproductive strategy increases
47 the survival rate of the offspring.

48 From the vernal equinox, the photoperiod begins to increase gradually, which
49 stimulates the secretion of prolactin from the pituitary gland[2] and initiates the
50 development of the corpus luteum, which, in turn, promotes an increase in
51 progesterone (P₄) secretion[3, 4]. When the level of P₄ in the body reaches the
52 requirement for blastocyst attachment to the uterine wall, the blastocysts begin to
53 implant and enter the fetal developmental period[4]. Since the embryos maintain only
54 basic metabolism during diapause, there is almost no mitosis or protein synthesis. The
55 embryo is thus in a free state within the uterus[3].

56 The uterus is the most important environment for embryonic development and
57 diapause, so the uterus and intrauterine substances play an important role in the
58 diapause and in reactivating of the embryo. In a recent study, the effects of
59 polyamines on diapaused mink embryos was validated. Treatment of mink uterine
60 epithelial cells with different doses of prolactin revealed that this hormone induces the
61 expression of polyamine regulatory genes such as *ODC1* in the uterus through the
62 pSTAT1 and mTOR pathways, thereby regulating the levels of polyamine in the
63 uterus[5]. In order to determine whether polyamines can alleviate embryo diapause,
64 embryos in diapause were incubated *in vitro* with putrescine, resulting in an increase
65 in blastocyst volume and the total number of cells, as indicated by further
66 development of embryos; non-treated control embryos, however, remained in a
67 diapause state[5]. Together, these results provide strong evidence showing that
68 embryos are maintained in a diapause state because of a restricted supply of
69 uterine-derived polyamines.

70 Differential gene expression has been observed between mink embryos in
71 diapause and reactivation mode. Over 200 embryonic genes were up-regulated during
72 activation. Expression of embryonic genes related to polyamine synthesis increased
73 during reactivation. Of the sequences corresponding to the genes characterized, about
74 14% were related to the cell cycle, and 14% were related to metabolism[5]; therefore,
75 it can be inferred that metabolism may play an important role in the process of
76 embryonic diapause and reactivation. Furthermore, as far as we know, no studies have
77 investigated the changes in the metabolome of minks before and after embryo
78 diapause.

79
80 Metabolomics an important component of systems biology. It is the science that
81 studies the interactions between endogenous metabolites and internal or external
82 factors in whole organisms, systems, organs, and cells[6]. Metabolomic analysis
83 techniques consist of gas or liquid chromatography coupled to mass spectrometry
84 (GC-MS/LC-MS), infrared spectroscopy (IR), and nuclear magnetic resonance
85 (NMR). Among these technologies, LC/MS is advantageous because of its high
86 resolution, high sensitivity, and reproducibility. Consequently, it has been widely used
87 for the identification and quantification of metabolites[7]. It is used to identify and
88 quantify hundreds of metabolites with high mass accuracy for comprehensive
89 metabolic profiling[8]. Here, we examined changes in the chemical composition of
90 the serum extracts taken during the different stages of pregnancy. Dopamine and
91 several amino acids can be used as markers for embryo diapause and reactivation. To
92 the best of our knowledge, no study has analyzed the metabolic changes taking place
93 from fertilization to embryo diapause, from embryo diapause to embryo reactivation,
94 during development, and during implantation. Our research is intended to support
95 scientific progress in this important field.

96 **2 Materials and Methods**

97 **2.1 Animals and serum collection**

98 All experiments on minks were guided by and with the approval of the Animal
99 Protection and Utilization Committee of Jilin University. Twenty multiparity minks
100 were farmed in the Special Economic Animal Experiment Base of the Chinese
101 Academy of Agricultural Sciences in Changchun (Jilin Province, P.R. China). All
102 minks were raised under conditions of controlled temperature (22–24°C) and
103 humidity (60–70%), where they were provided with sufficient food and water. Each
104 female mink was mated with a fertile male according to usual practice. Venous blood
105 from the 20 female minks was taken one day (D1), eight days (D8), 15 days (D15), 22
106 days (D22), and 29 days (D29) after mating. The blood was marked and transported at
107 2–8°C to the laboratory, centrifuged at 15,000 x g for 15 min, and the serum was
108 stored at –80°C until analysis. The 20 minks were fed and observed continually after
109 blood collection until the end of pregnancy. Of the 20 minks used, 15 subsequently
110 gave birth. Serum samples from six minks that shared the same gestation period (41
111 days) were ultimately used for metabolomic analysis. Six minks sera as three

112 biological replicates. The two sera of each sampling day were mixed for metabolomic
113 profiling.

114 **2.2 Sample preparation**

115 A serum sample (100 μ L) was placed in an EP tube, to which 300 μ L of
116 methanol and 20 μ L internal standard substances were added, followed by vortexing
117 for 30 sec. The samples were treated with ultrasound for 10 min (while incubated in
118 ice water) and then incubated for 1 h at -20°C to precipitate proteins. The sample was
119 then centrifuged at 15,000 x g for 15 min at 4°C . The supernatant (200 μ L) was
120 transferred into a fresh 2 mL LC/MS glass vial, 20 μ L were taken from each sample
121 and pooled together as QC samples. An additional 200 μ L of supernatant were taken
122 for UHPLC-QTOF-MS analysis.

123 **2.3 LC/MS analysis**

124 Metabolomic analysis was performed using an Agilent 1290 ultra-performance
125 LC system coupled to quadrupole time-of-flight (Triple TOF 5600 AB Sciex) mass
126 spectrometer, which is capable of performing primary and secondary mass
127 spectrometry data acquisition based on the IDA function under the control of Analyst
128 TF 1.7 software (AB Sciex). A UPLC BEH Amide column from Waters (1.7
129 $\mu\text{m} \times 2.1 \times 100$ mm) was used for chromatographic separation; the column temperature
130 was maintained at 40°C . The LC-MS system was run in a binary gradient solvent
131 mode. Solvent A contained 25 mM ammonium acetate and 25 mM ammonium
132 hydroxide in water (pH 9.75), and solvent B contained 0.1% formic acid in
133 acetonitrile. The flow rate was 500 $\mu\text{L}/\text{min}$. The linear gradient was as follows: 0 min,
134 95% B; 7 min, 65% B; 9 min, 40% B; 9.1 min, 95% B; 12 min, 95% B (Table 1).
135 Sample analysis was performed using the positive or negative electrospray ionization
136 (ESI) mode; the injection volume was 3 μL . In each cycle, twelve precursor ions with
137 an intensity greater than 100 were chosen for fragmentation at a collision energy (CE)
138 of 30 V (15 MS/MS events with a production accumulation time of 50 ms each). The
139 ESI ion source parameters were set as follows: ion source gas 1 at 60 psi, ion source
140 gas 2 at 60 psi, curtain gas at 35 psi, source temperature 650°C , ion spray voltage
141 floating (ISVF) 5,000 V or -4000 V in positive or negative modes, respectively.

142 Quality control (QC) samples, which were prepared by mixing equal volumes
143 (20 μL) from each serum sample as they were aliquoted for analysis, were used to
144 assess the reproducibility and reliability of the LC-MS system.

145 **2.4 Data processing and pattern recognition**

146 Unprocessed mass spectrometry data were converted to mzXML using
147 ProteoWizard software and then processed with the R package XCMS v3.2.). The
148 pre-processing results generated a data matrix that consisted of the retention time
149 (RT), mass-to-charge ratio (m/z) values, and peak intensity. The R package
150 CAMERA was used for peak annotation after XCMS data processing.

151 The resulting scaled datasets were applied to the principal component analysis
152 (PCA), which was used to validate the quality of the analytical system performance
153 and to observe possible outliers. The orthogonal projections to latent
154 structures-discriminant analysis (OPLS-DA) was used to analyse the results by
155 SIMCA-P v11.0 software (Umetrics AB, Umea, Sweden) to filter out orthogonal
156 variables in metabolites that are not related to categorical variables, and to analyse
157 non-orthogonal variables and orthogonal variables separately to obtain an overview of
158 the complete data set, and to discriminate between variables that are responsible for
159 variation between the groups. OPLS-DA score plots were used to evaluate the quality
160 of the model by the relevant R2 and Q2 parameters. The differential metabolites were
161 selected by the combination of the P-value of the ANOVA and variable importance in
162 the projection (VIP) values of the OPLS-DA model. The *P*-value was less than 0.05,
163 and the VIP value was larger than 1. The log2-fold change was used to show how
164 these selected differential metabolites varied between groups. Metabolites that varied
165 were also shown by Volcano Plot. The online database KEGG
166 (<http://www.genome.jp/kegg/>) was used to annotate the potential differential
167 metabolites by searching for the exact molecular mass data from redundant m/z peaks
168 against a specific metabolite. Metabolomic analyses were performed by SPSS v22.0
169 software.

170 **3 Results**

171 **3.1 Original chromatogram based on LC /MS**

172 All sample analyses were performed in positive and negative electrospray
173 ionization (ESI) mode by using ultra-performance LC quadrupole time-of-flight
174 tandem MS (UPLCQ-TOF-MS). A total of 849 metabolites were detected in positive
175 ion mode, 853 metabolites in negative ion mode (Supplement 1). A broad overlapping
176 spectrum of QC samples showed that the instrument has repeatability and stability
177 (Fig. 1).

178 **3.2 Multivariate statistical analysis**

179 PCA and orthogonal partial least-squares discriminant analysis (OPLS-DA) was
180 performed on the data from the 15 samples (five stages × three biological replicates)
181 to observe differences in metabolic profiles among different time points. The analysis
182 showed that there was a clear separation between D1 and another group in the
183 PD1×PD8 score plots (Fig. 2). To further search for ion peaks that discriminated
184 between the two groups, a supervised OPLS-DA model was established because it
185 focused on actual class discrimination more than the unsupervised PCA model. As
186 shown in Fig. 3, all R2X were greater than 0.5, R2Y was 1 or 0.999, and Q2 was
187 greater than 0.9, except D1 vs D8 in positive ion mode, indicating that the OPLS-DA
188 model had high predictive ability. The OPLS-DA models discriminated adequately
189 between different groups, both in positive and negative ion modes, which indicated
190 that their metabolic characteristics were distinct. To validate the reliability of the
191 OPLS-DA model, an alignment verification was performed (Fig. 4). R2' and Q2' were
192 lower than R2 and Q2 of the original model, which implies that the corresponding

193 points did not exceed the corresponding lines, indicating that the model was
194 meaningful. Thus, the differential metabolites can be screened according to the VIP.

195 **3.3 Identification of Potential Biomarkers and Metabolic Pathways**

196 In the first instance, metabolites with a VIP value greater than 1 in the OPLS-DA
197 model were selected. The ANOVA was used to select metabolites with significant
198 changes ($P < 0.05$). A volcano plot (Fig. 5) revealed differences in expression levels
199 of the metabolites in the two groups and the metabolites with statistically significant
200 differences. A total of 33 and 49 differential metabolites of the comparison group 1
201 (D1 VS D8) could be annotated in positive mode and negative mode using the KEGG
202 pathway database (Supplement 2). Most of the differentially-expressed amino acids
203 annotated were down-regulated, including L-proline, L-threonine, taurine, L-leucine,
204 D-ornithine, L-lysine, L-valine, L-kynurenine, and L-Glutamine. On the contrary,
205 L-methionine, L-phenylalanine, and L-tyrosine were up-regulated in D8 as compared
206 to D1. Similarly, dopamine and its precursor, tyramine, were significantly increased
207 in D8 as compared to D1 (Table 2). According to the KEGG pathway database, 38
208 metabolites were annotated (Supplement 3) in positive mode and 61 in negative mode
209 as differential metabolites of group 2 (D1 VS D15), more than half of which were the
210 same for group 1 (D1 VS D8). Levels of tyrosine and dopamine in D8 and D15 were
211 significantly higher than in D1, which is involved with the prolactin signaling
212 pathway. Almost the types of amino acids that up-regulated or down-regulated are the
213 same when compared to D8 and D15 with D1. Regarding group 3 (D1 VS D22), 45
214 differential metabolites in positive mode and 50 in negative mode were annotated
215 (Supplement 4). As for group 4 (D1 VS D29), 31 and 38 differential metabolites,
216 respectively, in the positive and negative ion modes were members of metabolic
217 pathways (Supplement 5). All amino acids were down-regulated on D22 as compared
218 to D1, except L-methionine and L-phenylalanine, and L-phenylalanine on D29.
219 Prolactin can induce polyamine synthesis, which is essential for embryo reactivation
220 [9]; moreover, dopamine is the primary physiological inhibitor of prolactin
221 secretion[10]. The higher the levels of dopamine on D8 and D15 indicated that the
222 embryos were in diapause. The interval from implantation to parturition in mink lasts
223 28-30 days[11, 12]. In our study, the intervals between the fourth blood sampling time
224 (D22) to labor lasted less than 30 days for all six minks, which indicated that the
225 embryos had already escaped from diapause and had implanted on D22, and it was
226 mid-pregnancy on D29. Therefore, further comparative analysis was conducted for
227 D8 vs D15 and D15 vs D22 with PCA and OPLS-DA. The data showed that there was
228 a clear separation between D8 and D15, D15, and D22 in the PD1×PD8 score plots
229 (Fig. 2S). For a more in-depth search for ion peaks that discriminated between the two
230 groups, the supervised OPLS-DA model was established. As shown in Fig. 3S, the
231 OPLS-DA model was highly predictive. To validate the reliability of the OPLS-DA
232 model, an alignment verification was performed (Fig. 4S). R2' and Q2' were smaller
233 than R2 and Q2 of the original model, indicating that the model was meaningful.
234 Differential metabolites could be screened according to the VIP. Metabolites with a
235 VIP value greater than 1 in the OPLS-DA model were selected, and the ANOVA was

236 used to select metabolites with significant changes ($P < 0.05$). Because many amino
237 acids promote mouse embryo development and blastocyst activation[13, 14], we
238 focused on the differential amino acids and dopamine in the different groups.
239 Dopamine was significantly higher on D15 than on D8, and the tyramine and
240 L-tyrosine, precursors of dopamine, were also higher on D15 than on D8, but
241 L-glutamine and D-ornithine decreased. L-lysine, L-arginine, L-kynurenine,
242 DL-phenylalanine, and L-phenylalanine were significantly upregulated on D15
243 compared to D8, while L-proline, taurine, and L-methionine increased slightly, but
244 the difference was not significant (Table 3). Dopamine and its precursors, tyramine,
245 and L-tyrosine decreased significantly on D22 as compared to D15, and most amino
246 acids were also down-regulated, including L-tyrosine, L-proline, D-ornithine, L-lysine,
247 L-leucine, L-tryptophan, DL-phenylalanine, and L-kynurenine; only L-glutamine and
248 L-pyroglutamic acid increased significantly (Table 4).

249 **4 Conclusion**

250 This study investigates aspects of metabolism of the female American mink
251 (*Neovison vison*). After fertilization, the mink blastocyst enters a stage of diapause
252 before it is reactivated and enters into a developmental stage in the uterus. The
253 reasons for this are probably related to availability of food sources and other
254 environmental conditions. The specific processes controlling embryo diapause and
255 reactivation have not previously been studied in the mink. Our aim was to identify
256 key metabolites associated with embryonic diapause and reactivation. We compared
257 blood serum metabolites at different stages in the pregnancy. The study makes a
258 significant contribution to the literature as we found that dopamine is a strong
259 candidate as an inhibitor of embryo reactivation. The study showed that levels of
260 seven amino acids, but especially L-leucine, may be correlated with embryo
261 reactivation.

262 **5 Discussion**

263 Dopamine is a precursor of noradrenaline and is involved in controlling fine
264 movements and mental processes. Mink require mating to stimulate ovulation, and the
265 fertilized eggs are formed 48-60 hours after mating. A fertilized egg takes about six
266 days to form a blastocyst and reach the uterus. The embryo does not implant
267 immediately but undergoes a period of cell cycle arrest[1]. As a result, oocyte
268 maturation or fertilization occurs one day after mating (D1), and the eighth day (D8)
269 may be the embryo diapause period. Dopamine levels significantly increased in D8 as
270 compared to D1, confirming that the blastocysts on D8 were in developmental arrest.
271 This suggests that dopamine levels may be a biomarker of mink embryonic diapause.
272 Similarly, dopamine concentration was higher on D15 than on D1, indicating that the
273 embryos of D15 were also in diapause. Tyrosine and tyramine, precursors of
274 dopamine, were also higher on D8 and D15 than on D1. It has been demonstrated that
275 CYP2D6 can mediate the derivation of dopamine from tyramine, while tyrosine
276 hydroxylase mediates the derivation of dopamine from tyrosine and that both tyrosine

277 and tyramine can increase dopamine levels[15]. L-phenylalanine is a synthetic
278 precursor of dopamine[16],which also impacts mouse embryo implantation negatively
279 by disrupting cytokine-based immunity and oxidative stress in the uterus[17].The
280 higher level of L-phenylalanine in the embryo of diapause stages D15 and D8 may
281 have negative effects on polyamine synthesis and embryo implantation. We also
282 found that dopamine and its precursors, L-phenylalanine, tyramine, and L-tyrosine,
283 were increased on D15 as compared to D8, further indicating that the embryo
284 diapause period was also occurring on D15. Dopamine and its precursors were lower
285 on D22 than on D15, indicating that embryos on D22 had implanted, which was
286 consistent with the suggestion that dopamine is a marker for mink embryo diapause.

287 In our study, The gestation period of minkis 41 days, we speculate that D15 may
288 be the end of embryo diapause. Thus, increasing amino acid levels may be a precursor
289 of embryo activation. Most amino acids increased to higher levels on D15 than on D8,
290 notably L-kynurenine, L-lysine, and L-arginine, which are precursors of polyamine.
291 After embryo implantation (D22), most amino acids decreased significantly as
292 compared to D15 and D1, indicating that amino acids may play an important role in
293 mink oocyte maturation and embryo reactivation. The levels of almost all amino acids
294 were reduced to a greater extent after embryo implantation (D22) than at the end of
295 the embryo diapause (D15), suggesting that the function of the amino acids may have
296 already been completed, leaving no further need for high concentrations of amino
297 acids after embryo reactivation.

298 As a major macronutrient, amino acids are not only a component of proteins and
299 peptides, but they are also essential for the synthesis of many biologically active
300 molecules involved in the regulation of signalling pathways and metabolism in the
301 body. Experimental evidence demonstrates that amino acids play a key role in female
302 and male reproduction[18, 19]. Many *in vitro* studies on mouse embryos have
303 demonstrated that amino acids, especially essential amino acids, have a vital role in
304 embryo development and blastocyst activation[9]. The embryonic development and
305 implantation requirements of amino acids are not simply nutritive to support protein
306 synthesis and trophoblast differentiation, but it also induces activation of
307 mTOR-dependent signals after the embryo has reached the early blastocyst stage. The
308 resultant signals cause transduction cascades, including triggering insulin-like growth
309 factor II and polyamine synthesis in the blastocyst, and finally increasing cell
310 motility[14, 20]. While polyamines are essential to folliculogenesis[21],
311 fertilization[22], and early embryo development[23, 24], deficiency of polyamines
312 causes embryo developmental arrest[9]. Most amino acids existed at greater levels on
313 D1 than on D8, D15, D22, and D29 demonstrating that amino acids may induce an
314 increase of polyamines via the mTOR pathway. Most amino acids annotated by the
315 KEGG pathway database, including L-proline, L-threonine, taurine, L-leucine,
316 D-ornithine, L-valine, and L-kynurenine, were down-regulated on D8 and D15 as
317 compared to D1. Our study showed that while polyamines are scarce during embryo
318 diapause[9], most amino acid levels were lower on D8 and D15 than on D1.
319 D-ornithine is a precursor of polyamine (putrescine), and arginine or proline can

320 synthesize putrescine through ornithine by the highly-regulated rate-limiting enzyme,
321 ornithine decarboxylase 1 (ODC1)[25].

322 Lower levels of D-ornithine and L-proline on D8 and D15 might cause a
323 decrease in putrescine synthesis, thereby hindering embryonic reactivation and
324 development. L-proline plays a novel role in the regulation of pluripotency and cell
325 differentiation, which can induce embryonic stem cells (ESC) to form early primitive
326 ectoderm-like cells[26]. In an *in vitro* mouse embryo culture, the omission of
327 L-threonine significantly reduces mouse blastocyst hatching, attachment, and
328 trophoblastic outgrowth[13]. L-threonine deprivation significantly decreases
329 self-renewal markers and differentiation markers of embryonic stem cells[27]. The
330 low concentrations of L-threonine on D8 and D15 coincided with the state of
331 embryonic diapause. Taurine can improve embryonic development *in vitro* in several
332 animals, including mouse[9], pig[28], cow[29], and rabbit[30]. What is more, taurine
333 is an osmotic adjustment organic substance[31, 32]. Therefore, it is nearly impossible
334 for taurine to spontaneously diffuse through the cell membrane because of its
335 lyophobic properties, and thus an extremely high intracellular concentration may be
336 maintained. Taurine acts as an osmolyte in human and mouse oocytes and embryos
337 when they have to adjust their cell volume because of either extracellularly-induced or
338 intracellularly-induced osmotic imbalances[33]. The low level of taurine on D8 and
339 D15 may be involved with mink blastocysts diapause, which is of no benefit to
340 blastocyst expansion and hatching. Human embryos that develop *in vitro* to the
341 blastocyst stage in the presence of amino acids always accumulate leucine, but not
342 other amino acids from the culture medium[34]. The decrease of leucine and valine
343 levels may be related to the diapause of the mink blastocyst.

344 The diapause period usually lasts 15-25 days, but sometimes, it is shortened to a
345 few days or extended up to 55 days[1, 35]. In hypophysectomised minks injected with
346 prolactin, embryo implantation occurred on days 14 and 21, but not at the same
347 time[36]. In our study, the interval from embryo diapause to implantation occurred
348 within seven days, indicating that a factor besides prolactin may be needed for the
349 blastocysts to escape from diapause and begin development, or, possible, that other
350 factors can accelerate embryo reactivation and implantation. The level of dopamine
351 was elevated, and the level of leucine was decreased during the diapause period of the
352 mink embryos. Changes in levels of dopamine and leucine may inhibit the production
353 of prolactin. Taken together, changes to amino acid levels on D8, D15, and D22
354 indicated that amino acids, especially leucine, may also be another important factor in
355 mink embryo diapause and reactivation. Leucine may have a synergistic effect with
356 prolactin during the activation of mink embryos, and an increase in both the levels of
357 leucine and prolactin may increase the rate of reactivation. Unfortunately, we did not
358 collect blood from the beginning of embryo development to test this. In addition,
359 these results need to be further verified by *in vitro* embryo culture and *in vivo*
360 experiments. These issues should be further studied by subsequent experiments so that
361 the mink embryo diapause and reactivation can be explored more comprehensively.

362 To the best of our knowledge, this is the first study to investigate links between
 363 serum metabolites and mink embryo diapause. The level of dopamine in the serum
 364 may be used as a marker for embryonic diapause, and changes in the levels of amino
 365 acids may be associated with embryo reactivation. This study fills a gap in
 366 metabolome analysis in this field and provides some references for subsequent
 367 research.

368 **6 Abbreviations**

369

Abbreviation	Meaning
P4	progesterone
GC-MS/LC-MS	gas or liquid chromatography coupled to mass spectrometry
IR	infrared spectroscopy
NMR	nuclear magnetic resonance
UHPLC-QTOF-MS	The ultra-high performance liquid chromatography-quadrupole time-of-flight mass spectrometry
QC	Quality control
ESI	negative electrospray ionization
OPLS-DA	orthogonal projections to latent structures-discriminant analysis
UPLCQ-TOF-MS	ultra-performance LC quadrupole time-of-flight tandem MS
ESC	embryonic stem cells

370

371 **7 Declaration**

372 **7.1 Ethical Approval and Consent to participate**

373 The study design was approved by the appropriate ethics review board. We have read
374 and understood your journal's policies, and we believe that neither the manuscript nor the
375 study violates any of these.

376 **7.2 Consent for publication**

377 All authors read and approved the final manuscript and, agree to the publication
378 of the manuscript.

379 **7.3 Availability of supporting data**

380 All data, models, and code generated or used during the study appear in the
381 submitted article.

382 **7.4 Conflict of Interest**

383 The authors declare that the research was conducted in the absence of any
384 commercial or financial relationships that could be construed as a potential conflict of
385 interest.

386 **7.5 Funding**

387 This research was supported by the National Key Research and Development
388 Program of China (2017YFD0501701), The National Natural Science Foundation of
389 China (31672417), and the Science and Technology Development Project of
390 Changchun (17DY022).

391 **7.6 Author Contributions**

392 All of the authors contributed to the conception of the review. CJL designed the
393 experiment, while ZL and LD performed the experiment. The first draft of the
394 manuscript was prepared by CL. CJL performed subsequent amendments. ZL revised
395 the manuscript. All authors read and approved the final manuscript.

396 **7.7 Acknowledgments**

397 We acknowledge the staff at the Special Economic Animal Experiment Base of
398 the Chinese Academy of Agricultural Sciences for their help in providing the animals
399 and collecting serum; as well as the staff at biomarker technologies for their excellent
400 technical assistance.

401 **8 References**

- 402 1. Murphy BD, James DA: **The effects of light and sympathetic innervation to**
403 **the head on nidation in mink.** *Journal of Experimental Zoology* 1974,
404 **187:267-276.**
- 405 2. Murphy B, DiGregorio G, Douglas D, Gonzalez-Reyna A: **Interactions**
406 **between melatonin and prolactin during gestation in mink (Mustela**
407 **vison).** *Reproduction* 1990, **89:423-429.**
- 408 3. Papke RL, Concannon PW, Travis HF, Hansel W: **Control of luteal function**
409 **and implantation in the mink by prolactin.** *Journal of Animal Science* 1980,
410 **50:1102-1107.**

- 411 4. Martinet L, Allain D, Meunier M: **Regulation in pregnant mink (*Mustela***
412 **vison) of plasma progesterone and prolactin concentrations and**
413 **regulation of onset of the spring moult by daylight ratio and melatonin**
414 **injections.** *Canadian journal of zoology* 1983, **61**:1959-1963.
- 415 5. Fenelon JC, Banerjee A, Lefèvre P, Gratian F, Murphy BD:
416 **Polyamine-mediated effects of prolactin dictate emergence from mink**
417 **obligate embryonic diapause.** *Biology of reproduction* 2016, **95**:6, 1-13.
- 418 6. Tang H, Wang Y: **Metabonomics: a revolution in progress.** *Sheng wu hua*
419 *xue yu sheng wu wu li jin zhan* 2006, **33**:401-417.
- 420 7. Zhou B, Xiao JF, Tuli L, Ressom HW: **LC-MS-based metabolomics.**
421 *Molecular BioSystems* 2012, **8**:470-481.
- 422 8. Theodoridis G, Gika HG, Wilson ID: **LC-MS-based methodology for global**
423 **metabolite profiling in metabonomics/metabolomics.** *TrAC Trends in*
424 *Analytical Chemistry* 2008, **27**:251-260.
- 425 9. !!! INVALID CITATION !!!
- 426 10. Massara F, Camanni F, Belforte L, Molinatti G: **Dopamine and inhibition of**
427 **prolactin and growth-hormone secretion.** *Lancet (London, England)* 1976,
428 **1**:913-913.
- 429 11. Enders RK: **Reproduction in the mink (*Mustela vison*).** *Proceedings of the*
430 *American Philosophical Society* 1952, **96**:691-755.
- 431 12. Concannon P, Pilbeam T, Travis H: **Advanced implantation in mink**
432 **(*Mustela vison*) treated with medroxyprogesterone acetate during early**
433 **embryonic diapause.** *Reproduction* 1980, **58**:1-6.
- 434 13. Spindle AI, Pedersen RA: **Hatching, attachment, and outgrowth of mouse**
435 **blastocysts in vitro: fixed nitrogen requirements.** *Journal of Experimental*
436 *Zoology* 1973, **186**:305-318.
- 437 14. Martin PM, Sutherland AE: **Exogenous amino acids regulate**
438 **trophectoderm differentiation in the mouse blastocyst through an**
439 **mTOR-dependent pathway.** *Developmental biology* 2001, **240**:182-193.
- 440 15. Zhu W, Mantione KJ, Shen L, Cadet P, Esch T, Goumon Y, Bianchi E, Sonetti
441 D, Stefano GB: **Tyrosine and tyramine increase endogenous ganglionic**
442 **morphine and dopamine levels in vitro and in vivo: cyp2d6 and tyrosine**
443 **hydroxylase modulation demonstrates a dopamine coupling.** *Medical*
444 *Science Monitor* 2005, **11**:BR397-BR404.
- 445 16. Kapatos G, Zigmond M: **DOPAMINE BIOSYNTHESIS FROM L-**
446 **TYROSINE AND L-PHENYLALANINE IN RAT BRAIN**
447 **SYNAPTOSOMES: PREFERENTIAL USE OF NEWLY**
448 **ACCUMULATED PRECURSORS 1, 2.** *Journal of neurochemistry* 1977,
449 **28**:1109-1119.

- 450 17. Dong Y, Bai Y, Liu G, Wang Z, Cao J, Chen Y, Yang H: **The immunologic**
451 **and antioxidant effects of L-phenylalanine on the uterine implantation of**
452 **mice embryos during early pregnancy.** *Histology and histopathology* 2014,
453 **29:1335-1342.**
- 454 18. Wu G, Bazer FW, Dai Z, Li D, Wang J, Wu Z: **Amino acid nutrition in**
455 **animals: protein synthesis and beyond.** *Annu Rev Anim Biosci* 2014,
456 **2:387-417.**
- 457 19. Bazer FW: **Contributions of an animal scientist to understanding the**
458 **biology of the uterus and pregnancy.** *Reproduction, Fertility and*
459 *Development* 2012, **25:129-147.**
- 460 20. Martin PM, Sutherland AE, Van Winkle LJ: **Amino acid transport regulates**
461 **blastocyst implantation.** *Biology of reproduction* 2003, **69:1101-1108.**
- 462 21. Bastida CM, Cremades An, Castells MT, López-Contreras AsJ, López-García
463 C, Tejada F, Peñafiel R: **Influence of ovarian ornithine decarboxylase in**
464 **folliculogenesis and luteinization.** *Endocrinology* 2005, **146:666-674.**
- 465 22. Fleming AD, Armstrong DT: **Effects of polyamines upon capacitation and**
466 **fertilization in the guinea pig.** *Journal of Experimental Zoology* 1985,
467 **233:93-100.**
- 468 23. Alexandre H: **Effect of inhibitors of polyamine biosynthesis on primary**
469 **differentiation of mouse egg.** *Comptes rendus hebdomadaires des seances de*
470 *l'Academie des sciences Serie D: Sciences naturelles* 1978, **286:1215-1217.**
- 471 24. Part M, Prakash N, Grove J, Schechter P, Sjoerdsma A, Koch-Weser J:
472 **L-Ornithine decarboxylase: an essential role in early mammalian**
473 **embryogenesis.** *Science* 1980, **208:505-508.**
- 474 25. Wallace HM, Fraser AV, Hughes A: **A perspective of polyamine**
475 **metabolism.** *Biochemical Journal* 2003, **376:1-14.**
- 476 26. Washington JM, Rathjen J, Felquer F, Lonic A, Bettess MD, Hamra N,
477 Semendric L, Tan BSN, Lake J-A, Keough RA: **L-Proline induces**
478 **differentiation of ES cells: a novel role for an amino acid in the regulation**
479 **of pluripotent cells in culture.** *American Journal of Physiology-Cell*
480 *Physiology* 2010, **298:C982-C992.**
- 481 27. Wang J, Alexander P, Wu L, Hammer R, Cleaver O, McKnight SL:
482 **Dependence of mouse embryonic stem cells on threonine catabolism.**
483 *Science* 2009, **325:435-439.**
- 484 28. Petters R, Wells K: **Culture of pig embryos.** *Journal of reproduction and*
485 *fertility Supplement* 1993, **48:61-73.**
- 486 29. Liu Z, Foote RH: **Development of bovine embryos in KSOM with added**
487 **superoxide dismutase and taurine and with five and twenty percent O₂.**
488 *Biology of reproduction* 1995, **53:786-790.**

- 489 30. Li J, Foote RH, Simkin M: **Development of rabbit zygotes cultured in**
490 **protein-free medium with catalase, taurine, or superoxide dismutase.**
491 *Biology of reproduction* 1993, **49**:33-37.
- 492 31. Huxtable R: **Physiological actions of taurine.** *Physiological reviews* 1992,
493 **72**:101-163.
- 494 32. McManus ML, Churchwell KB, Strange K: **Regulation of cell volume in**
495 **health and disease.** *New England Journal of Medicine* 1995, **333**:1260-1267.
- 496 33. Dumoulin JC, Wissen LCV, Menheere PP, Michiels AH, Geraedts JP, Evers
497 **JL: Taurine acts as an osmolyte in human and mouse oocytes and**
498 **embryos.** *Biology of Reproduction* 1997, **56**:739.
- 499 34. Hemmings K, Maruthini D, Vyjayanthi S, Hogg J, Balen A, Campbell B,
500 Leese H, Picton H: **Amino acid turnover by human oocytes is influenced**
501 **by gamete developmental competence, patient characteristics and**
502 **gonadotrophin treatment.** *Human Reproduction* 2013, **28**:1031-1044.
- 503 35. Martinet L, Allais C, Allain D: **The role of prolactin and LH in luteal**
504 **function and blastocyst growth in mink (*Mustela vison*).** *Journal of*
505 *reproduction and fertility Supplement* 1981, **29**:119.
- 506 36. Murphy BD, Concannon PW, Travis HF, Hansel W: **Prolactin: The**
507 **Hypophyseal Factor That Terminates Embryonic Diapause in Mink.**
508 *Biology of Reproduction* 1981, **25**:487.

509

510

511

Table 1 The gradient of the mobile phase.

Time (min)	Flow rate (µL/min)	A%	B%
0	500	5	95
0.5	500	5	95
7	500	35	65
8	500	60	40
9	500	60	40
9.1	500	5	95

Table 2 Amino acids and dopamine change (D1 VS D8)

NO.	name	log2 Fold Change(D8/D1)	P-value	VIP	regulated
1	L-Proline	-0.599	0.003	1.300	down
2	L-Valine	-0.703	0.004	1.294	down
3	L-Threonine	-0.656	0.015	1.225	down
4	Taurine	-0.467	0.049	1.201	down
5	L-Leucine	-0.381	0.021	1.204	down
6	L-Methionine	1.054	0.036	1.249	up
7	L-Phenylalanine	1.033	0.001	1.358	up
8	L-Glutamine	-0.334	0.030	1.198	down
9	Tyramine	0.982	0.022	1.474	up
10	Dopamine	0.682	0.000	1.543	up
11	D-Ornithine	-1.213	0.004	1.487	down
12	L-Tyrosine	0.916	0.000	1.535	up
13	L-Lysine	-0.576	0.002	1.518	down
14	L-Kynurenine	-0.551	0.000	1.533	down

Table 3 Amino acids and dopamine change (D8 VS D15)

NO.	name	log2 Fold Change(D15/D 8)	P-value	VIP	regulated
1	L-Proline	0.145	0.133	1.062	unchanged
2	Tyramine	0.535	0.012	1.266	up
3	Taurine	0.518	0.058	1.128	unchanged
4	Dopamine	0.456	0.000	1.379	up
5	L-Methionine	0.640	0.052	1.160	unchanged
6	L-Phenylalanine	0.702	0.036	1.246	up
7	D-Ornithine	-1.058	0.032	1.282	down
8	L-Tyrosine	0.347	0.002	1.364	up
9	L-Lysine	0.956	0.007	1.343	up
10	L-Kynurenine	0.397	0.018	1.283	up
11	DL-Phenylalanine	0.681	0.029	1.189	up
12	L-Arginine	0.175	0.045	1.215	up
13	L-Glutamine	-0.705	0.001	1.412	down

514

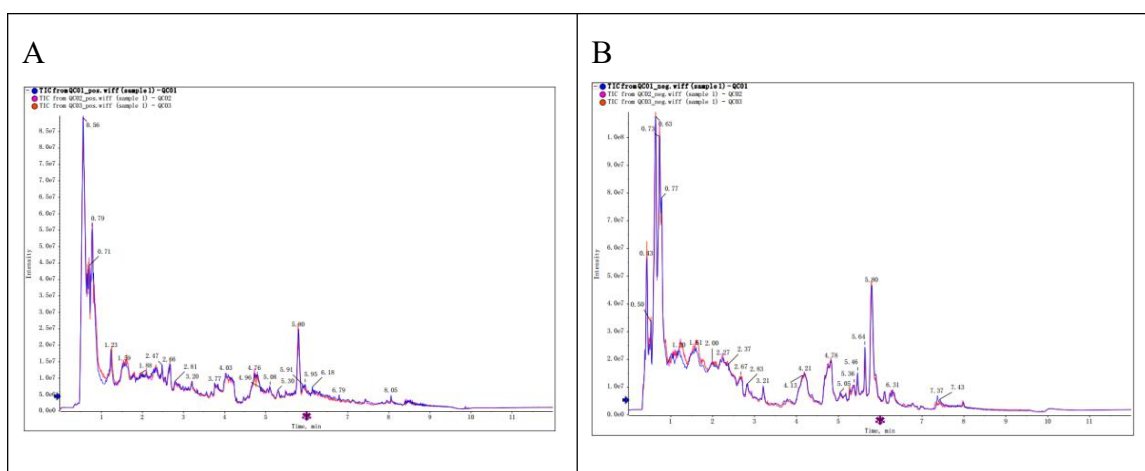
Table 4 Amino acids and dopamine change (D15 VS D22)

NO.	name	log2 Fold Change(D22/D	P-value	VIP	regulated
-----	------	---------------------------	---------	-----	-----------

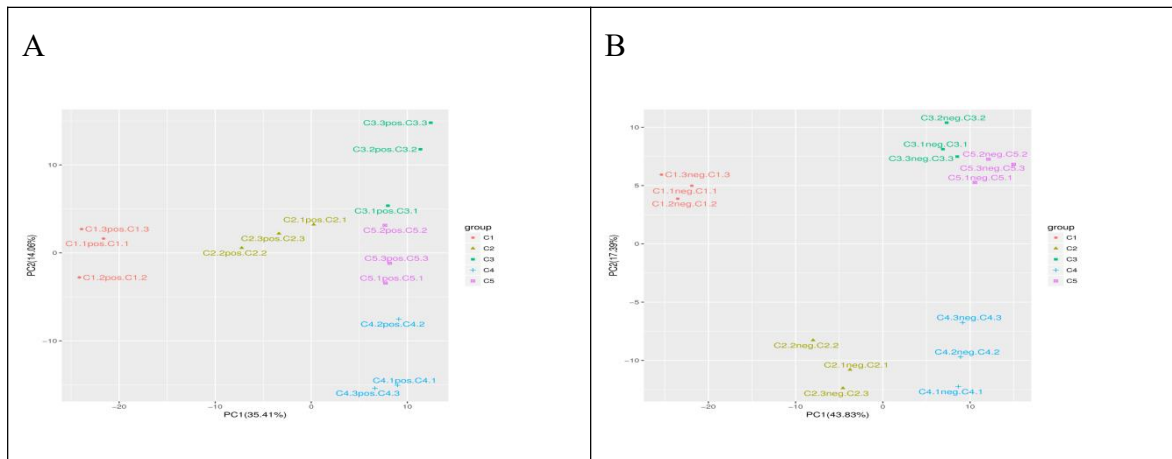
15)

1	L-Leucine	-0.263	0.038	1.268	down
2	L-Glutamine	0.512	0.010	1.374	up
3	L-Proline	-0.501	0.016	1.429	down
4	Tyramine	-0.353	0.035	1.370	down
5	D-Ornithine	-0.581	0.008	1.360	down
6	DL-Phenylalanine	-0.998	0.018	1.329	down
7	Dopamine	-0.993	0.008	1.464	down
8	L-Tyrosine	-0.961	0.033	1.402	down
9	L-Lysine	-0.556	0.023	1.387	down
10	L-Tryptophan	-0.535	0.023	1.325	down
11	L-Kynurenine	-0.891	0.002	1.449	down
12	L-Pyroglutamic acid	0.768	0.029	1.309	up

515



516 Fig. 1 Total Ion Chromatogram of QC in ESI+ mode (A) and ESI -mode (B)

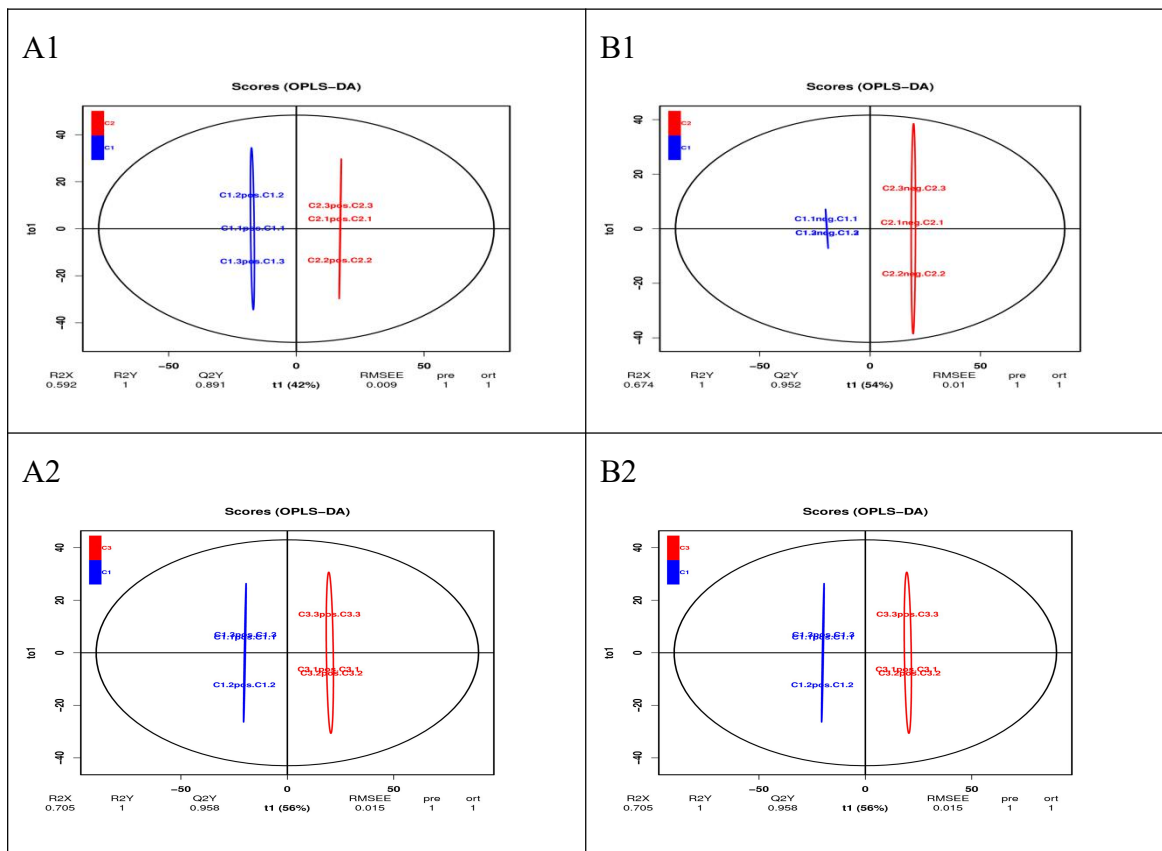


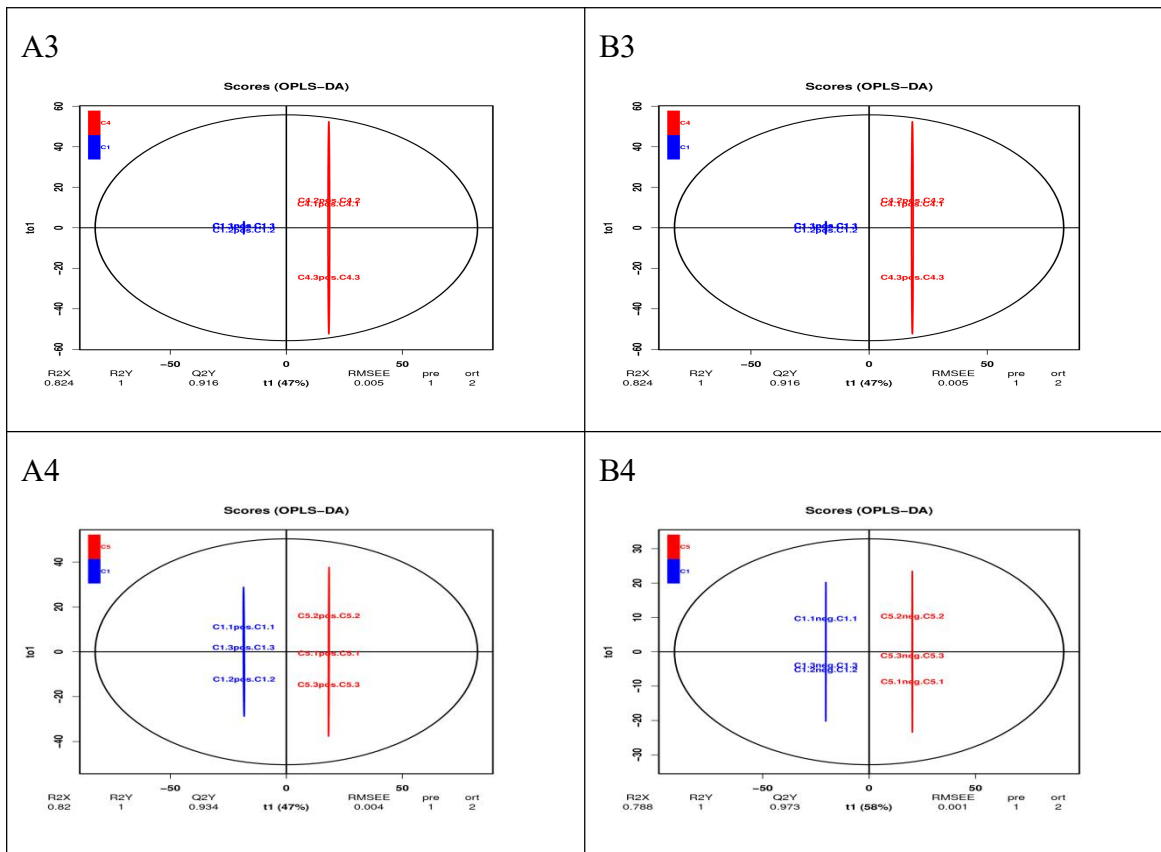
518 Fig. 2 PCA score plots in the five groups in ESI+ mode (A) and ESI- mode (B).

519

520

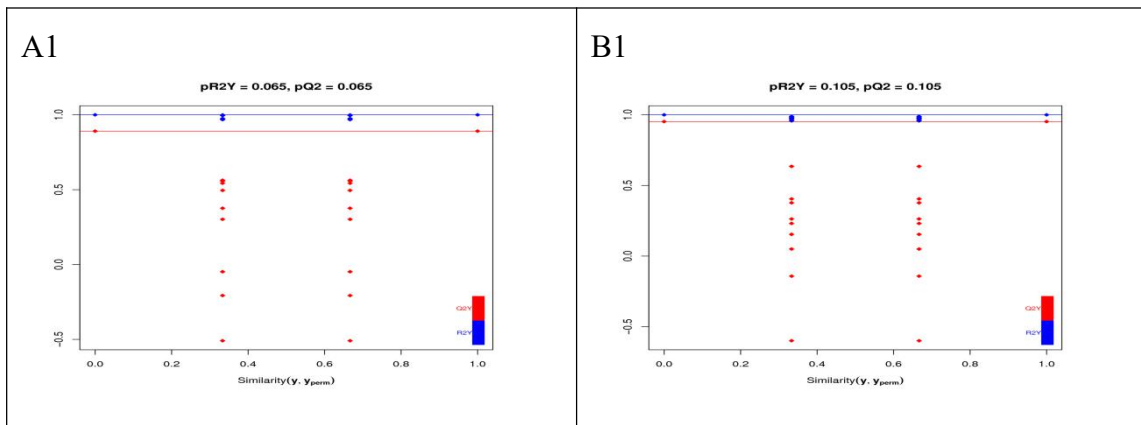
521

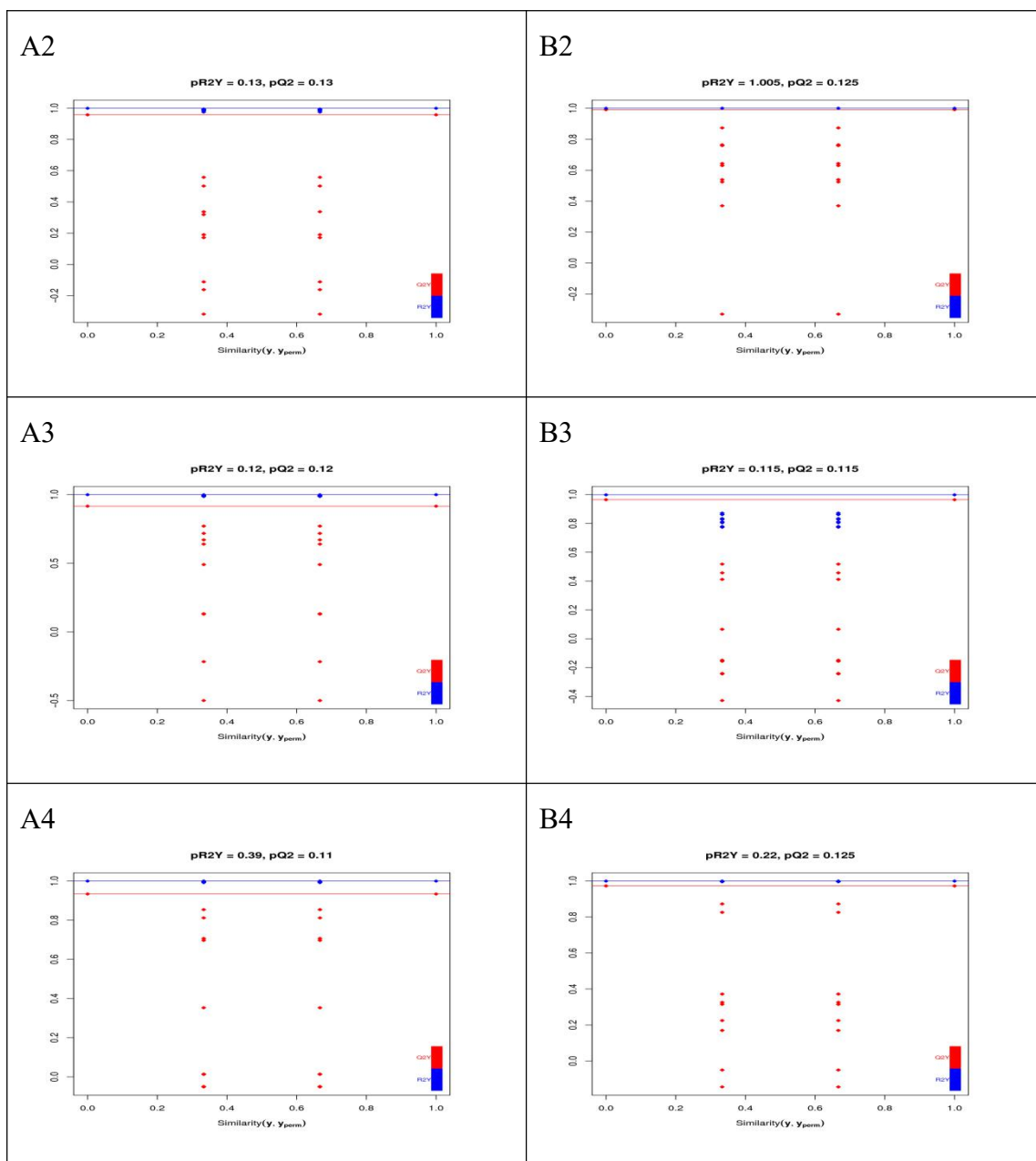




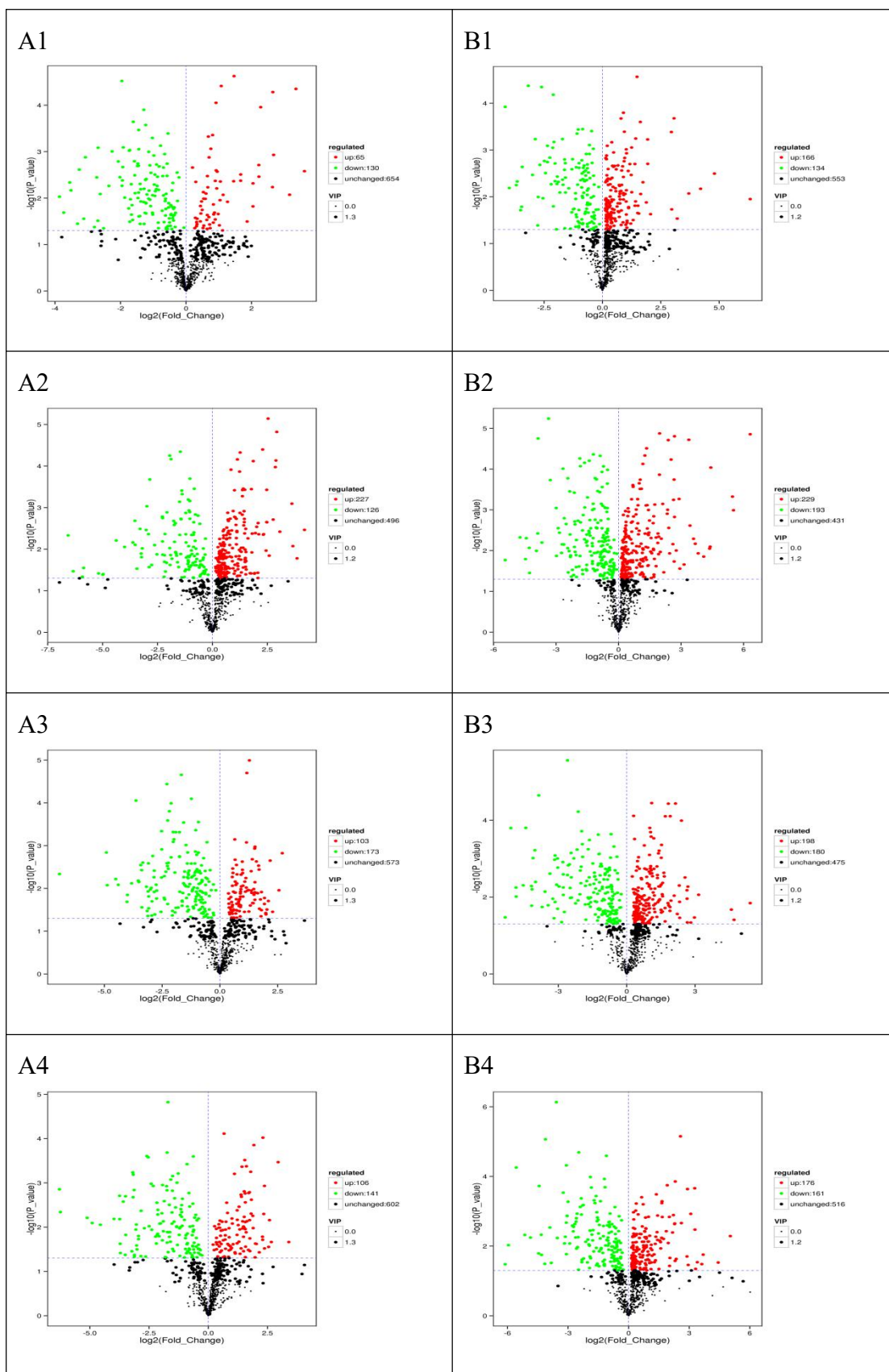
522

523 Fig. 3 OPLS-DA score plot of the four comparisons: (A1) D1 vs D8 in ESI+ mode,
 524 (B1) D1 vs D8 in ESI- mode; (A2) D1 vs D15 in ESI+ mode, (B2) D1 vs D15 in ESI-
 525 mode; (A3) D1 vs D22 in ESI+ mode, (B3) D1 vs D22 in ESI- mode; (A4) D1 vs D29
 526 in ESI+ mode, (B4) D1 vs D29 in ESI- mode.



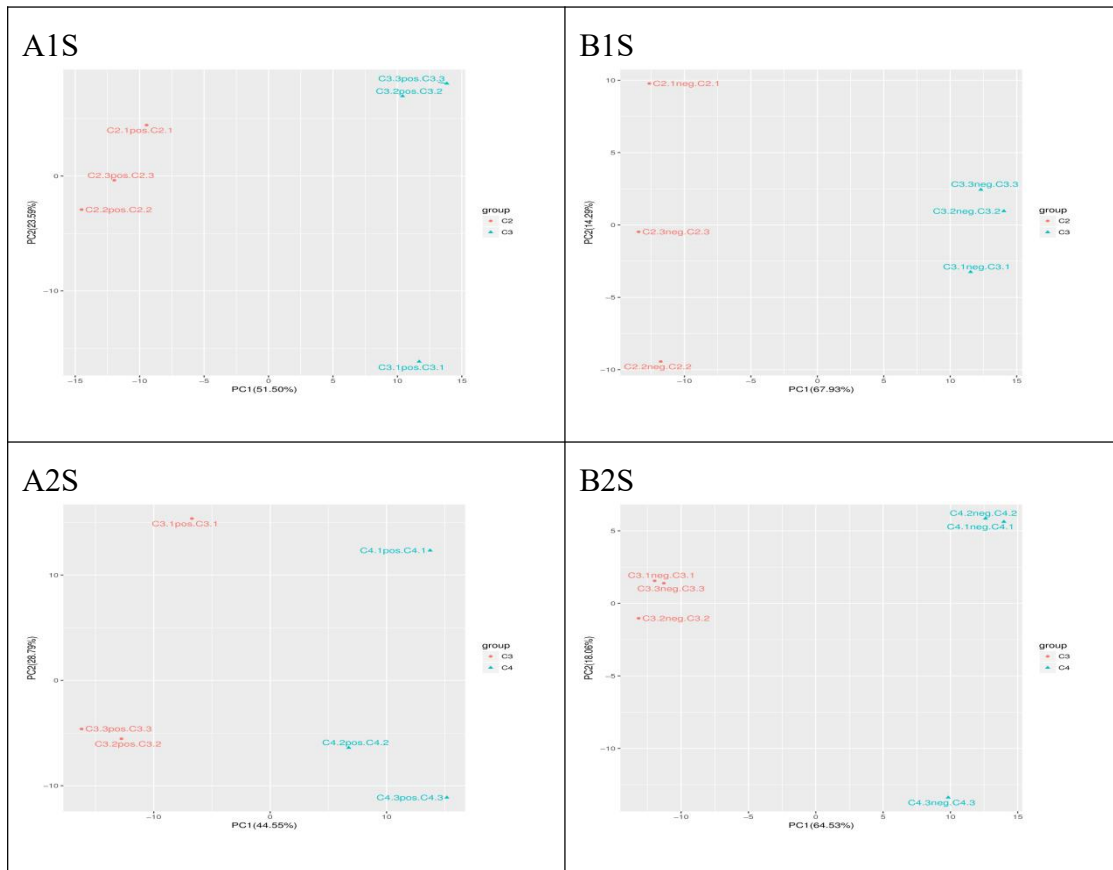


527 Fig.4 Validation plot of OPLS-DA model. The horizontal line corresponded to R2 and
 528 Q2 of the original model, and the blue point and red point represented R2' and Q2' of
 529 the model after Y replacement, respectively. (A1)D1 vs D8 in ESI+ mode, (B1) D1 vs
 530 D8 in ESI- mode; (A2) D1 vs D15 in ESI+ mode, (B2) D1 vs D15 in ESI- mode; (A3)
 531 D1 vs D22 in ESI+ mode, (B3) D1 vs D22 in ESI- mode; (A4) D1 vs D29 in ESI+
 532 mode, (B4) D1 vs D29 in ESI- mode.

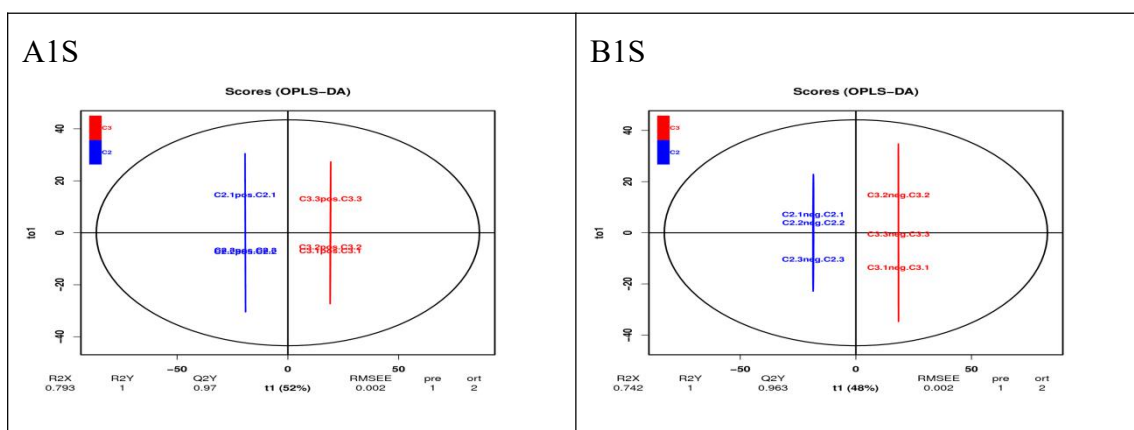


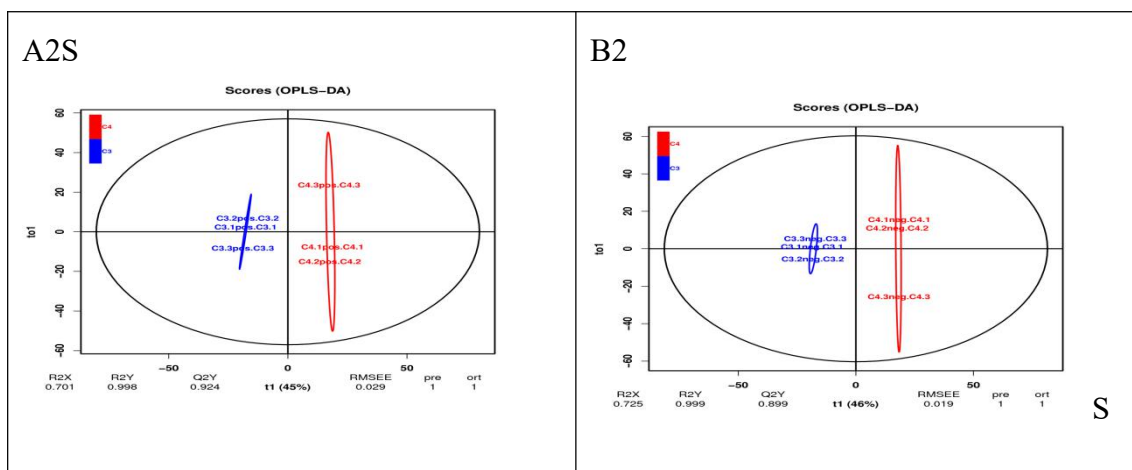
533 Fig. 5 Volcano Plot with differential metabolites of the four comparison groups. Each
 534 point in the figure represents a metabolite, the abscissa represents the log₂-fold
 535 change of the group compared to the substance, and the ordinate represents the

536 log₁₀-P-value of the student's t-test. The scatter size represents the VIP value of the
 537 OPLS-DA model. Green dots represent significantly down-regulated metabolites, red
 538 dots represent significantly up-regulated metabolites, and black dots represent
 539 metabolites detected but not significantly different. (A1) D1 vs D8 in ESI+ mode, (B1)
 540 D1 vs D8 in ESI- mode; (A2) D1 vs D15 in ESI+ mode, (B2) D1 vs D15 in ESI-
 541 mode; (A3) D1 vs D22 in ESI+ mode, (B3) D1 vs D22 in ESI- mode; (A4) D1 vs D29
 542 in ESI+ mode, (B4) D1 vs D29 in ESI- mode.



543 Fig. 2S PCA score plots in D8 vs D15, D15 vs D22 in ESI+ mode (A) and ESI- mode
 544 (B). (A1S) D8 vs D15 in ESI+ mode, (B1S) D8 vs D15 in ESI- mode; (A2S) D15 vs
 545 D22 in ESI+ mode, (B2S) D15 vs D22 in ESI- mode.



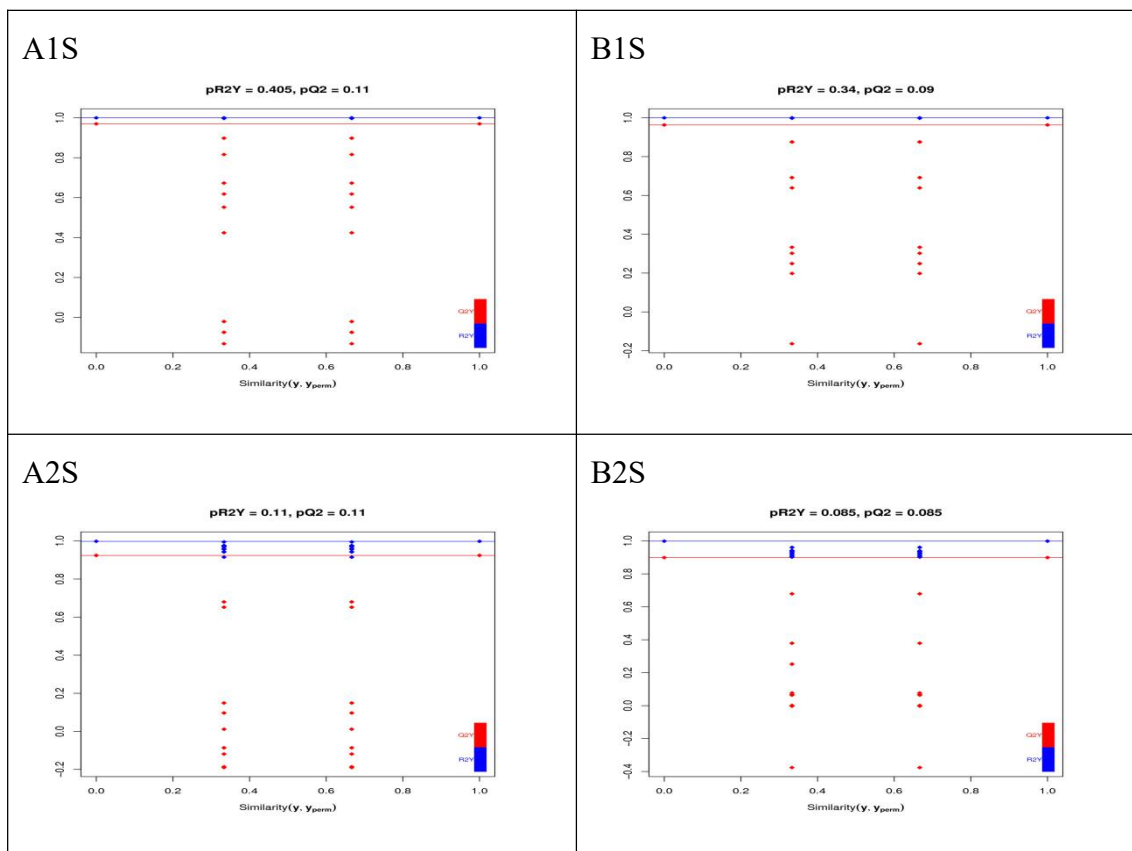


546 Fig. 3S OPLS-DA score plot D8 vs D15, D15 vsD22 in ESI+ mode (A) and ESI-
 547 mode (B). (A1S) D8 vsD15 in ESI+ mode, (B1S) D8 vs D15 in ESI- mode; (A2S)
 548 D15 vs D22 in ESI+ mode, (B2S) D15 vs D22 in ESI- mode.

549

550

551



552 Fig.4S Validation plot of OPLS-DA model D8 vs D15, D15 vsD22in ESI+ mode (A)
 553 and ESI- mode (B). The horizontal line corresponded to R2 and Q2 of the original

554 model, and the blue point and red point represented R2' and Q2' of the model after Y
555 replacement, respectively. (A1S) D8 vs D15 in ESI+ mode, (B1S) D8 vs D15 in ESI-
556 mode; (A2S) D15 vs D22 in ESI+ mode, (B2S) D15 vs D22 in ESI- mode.

557

558

559

560

561

562

563

564

Figures

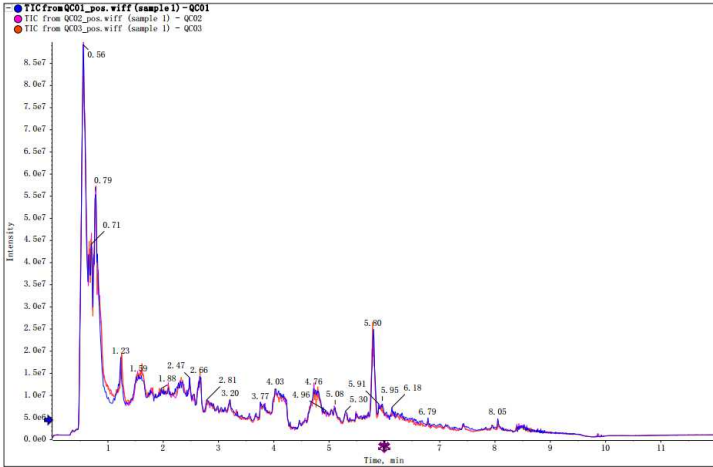


Fig. 1-A

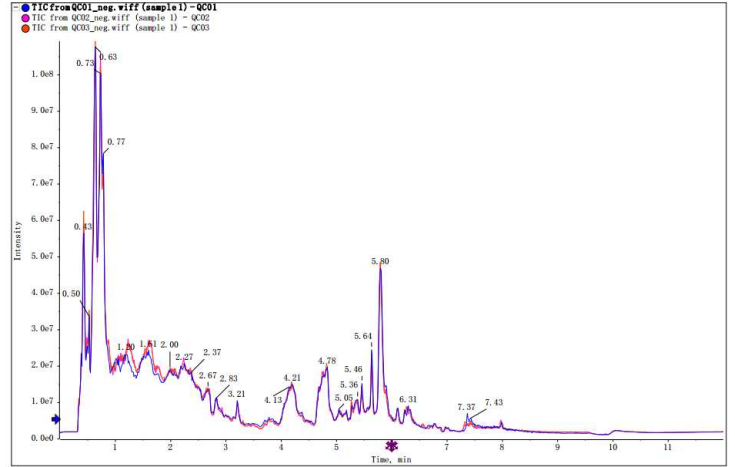


Fig. 1-B

Figure 1

Total Ion Chromatogram of QC in ESI+ mode (A) and ESI- mode (B)

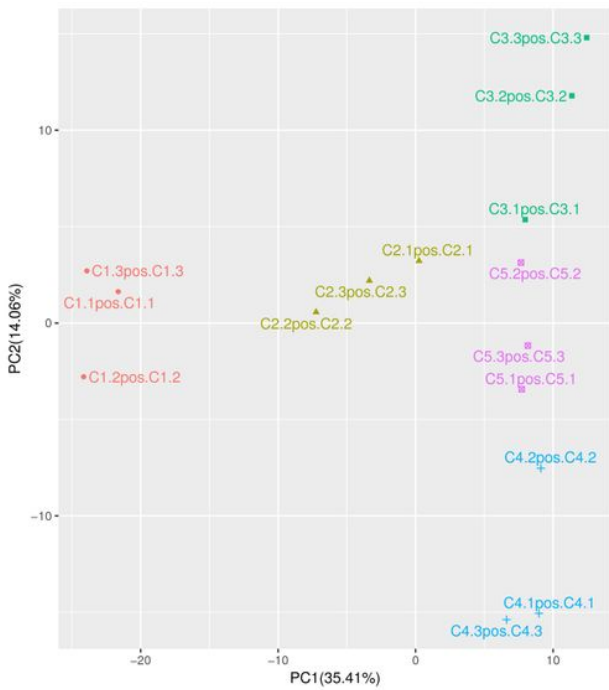


Fig. 2-A

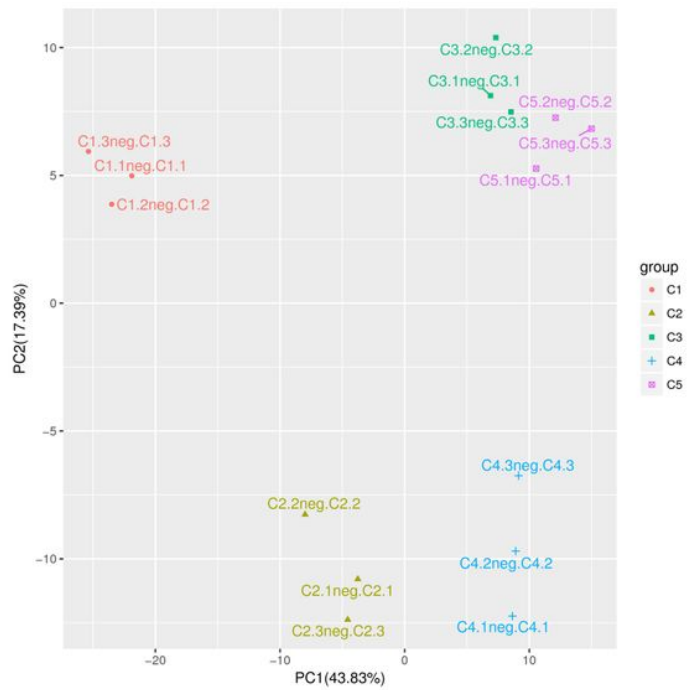


Fig. 2-B

Figure 2

PCA score plots in the five groups in ESI+ mode (A) and ESI- mode (B).

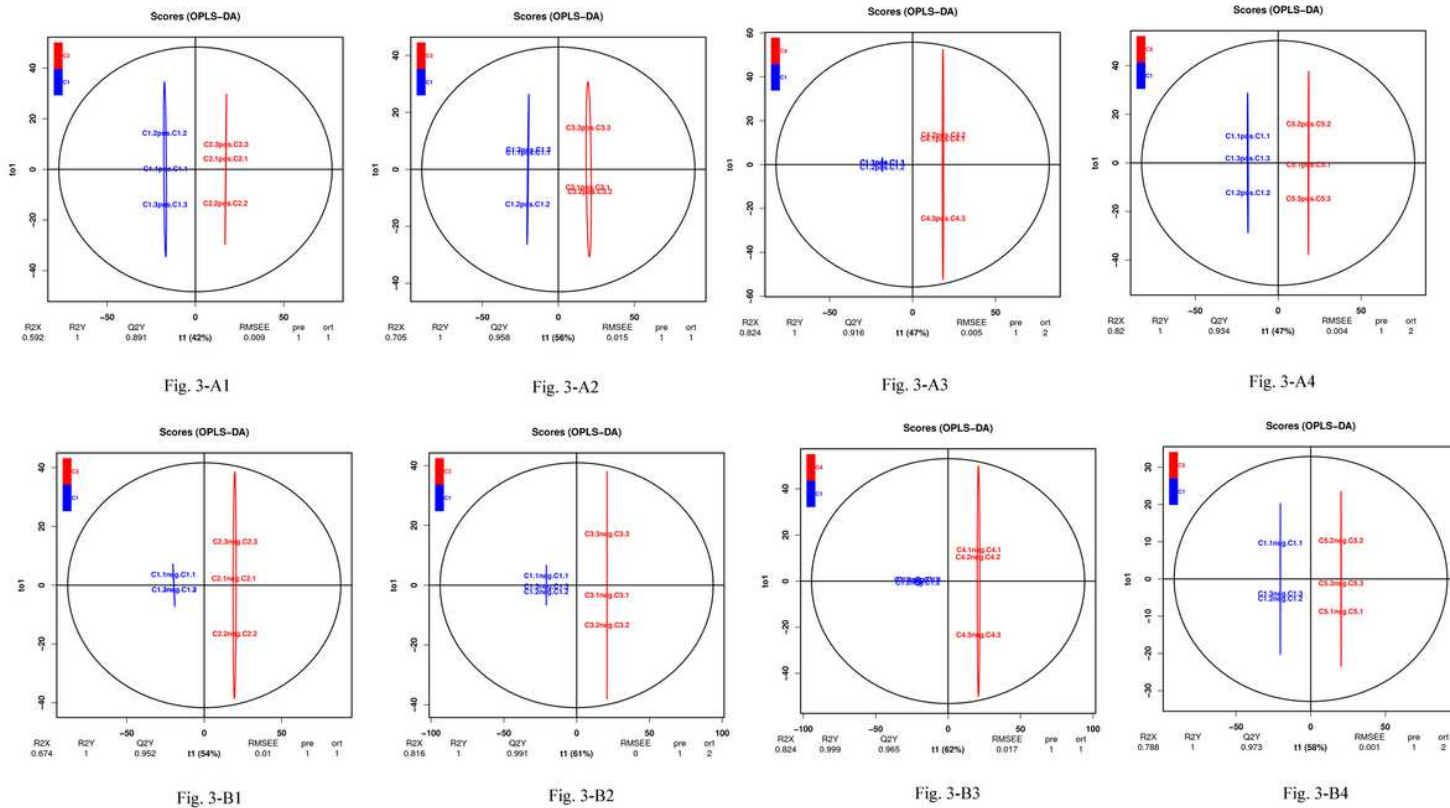


Figure 3

OPLS-DA score plot of the four comparisons: (A1) D1 vs D8 in ESI+ mode, (B1) D1 vs D8 in ESI- mode; (A2) D1 vs D15 in ESI+ mode, (B2) D1 vs D15 in ESI mode; (A3) D1 vs D22 in ESI+ mode, (B3) D1 vs D22 in ESI- mode; (A4) D1 vs D29 in ESI+ mode, (B4) D1 vs D29 in ESI- mode.

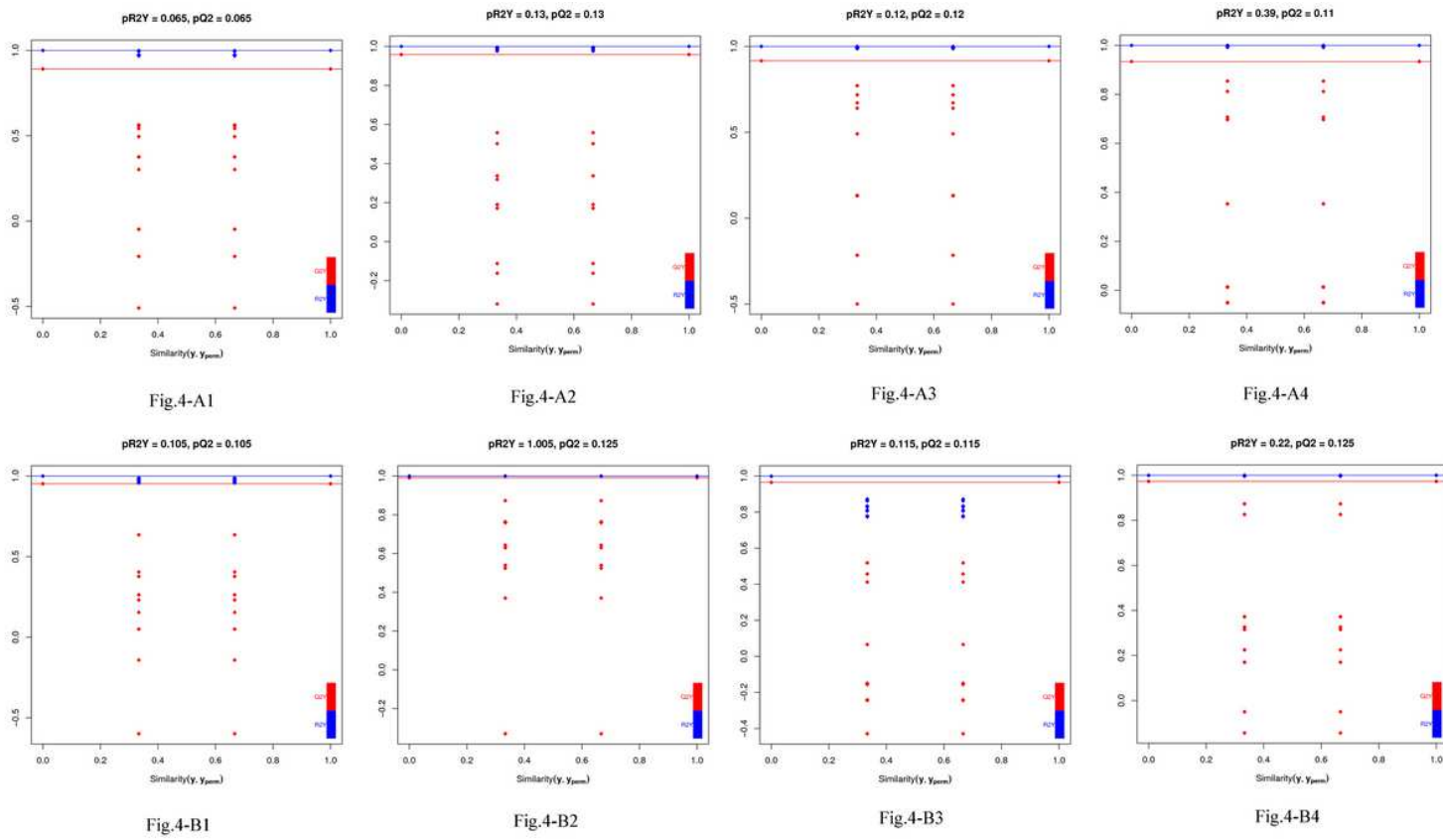


Figure 4

Validation plot of OPLS-DA model. The horizontal line corresponded to R² and Q² of the original model, and the blue point and red point represented R²' and Q²' of the model after Y replacement, respectively. (A1) D1 vs D8 in ESI+ mode, (B1) D1 vs D8 in ESI- mode; (A2) D1 vs D15 in ESI+ mode, (B2) D1 vs D15 in ESI- mode; (A3) D1 vs D22 in ESI+ mode, (B3) D1 vs D22 in ESI- mode; (A4) D1 vs D29 in ESI+ mode, (B4) D1 vs D29 in ESI- mode.

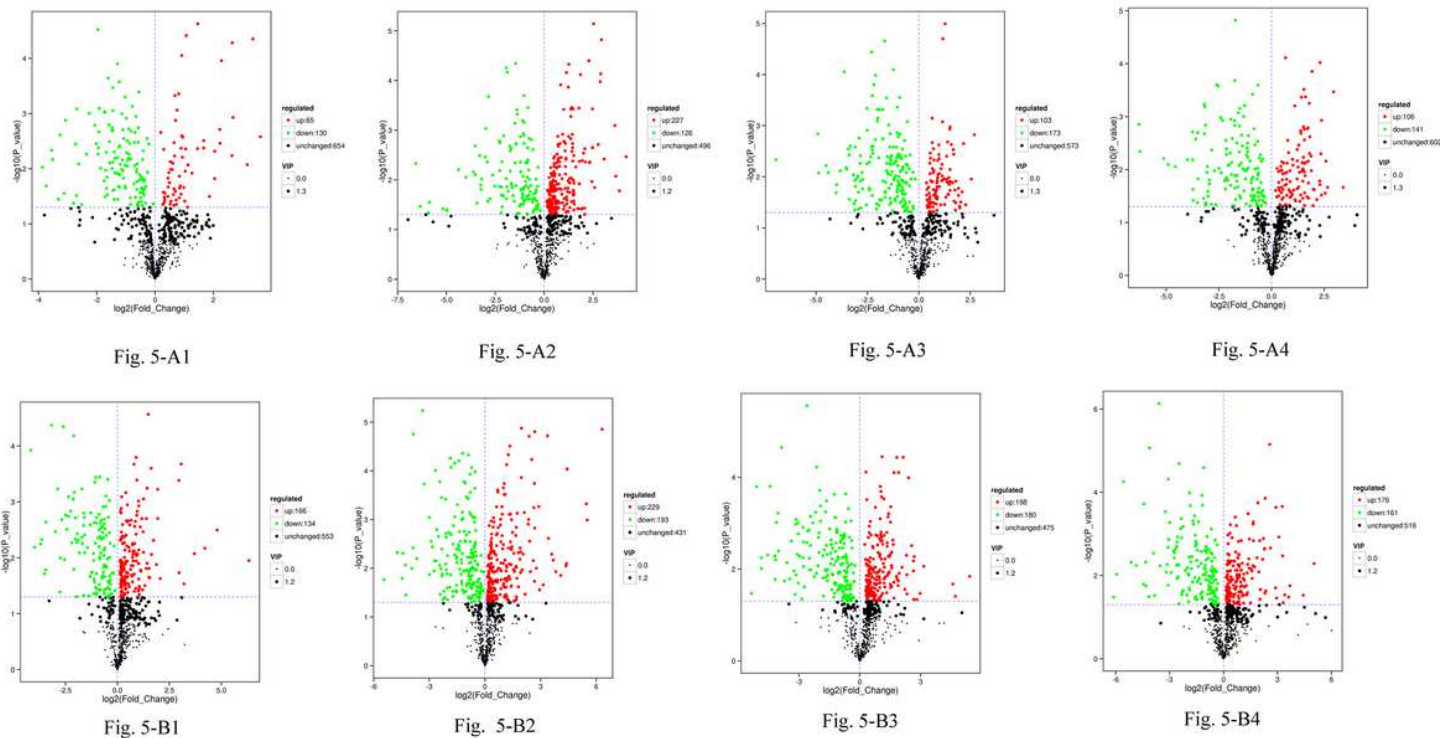


Figure 5

Volcano Plot with differential metabolites of the four comparison groups. Each point in the figure represents a metabolite, the abscissa represents the log₂-fold change of the group compared to the substance, and the ordinate represents the log₁₀-P-value of the student's t-test. The scatter size represents 536 the VIP value of the OPLS-DA model. Green dots represent significantly down-regulated metabolites, red dots represent significantly up-regulated metabolites, and black dots represent metabolites detected but not significantly different. (A1) D1 vs D8 in ESI+ mode, (B1) D1 vs D8 in ESI- mode; (A2) D1 vs D15 in ESI+ mode, (B2) D1 vs D15 in ESI mode; (A3) D1 vs D22 in ESI+ mode, (B3) D1 vs D22 in ESI- mode; (A4) D1 vs D29 in ESI+ mode, (B4) D1 vs D29 in ESI- mode.

Supplementary Files

This is a list of supplementary files associated with this preprint. Click to download.

- [supplement4D1vsD15..xls](#)
- [QCposTIC.png](#)
- [supplement5posD1vsD29.xls](#)
- [Fig4SA1A2B1B2.jpg](#)
- [Fig2SA1A2B1B2.jpg](#)
- [Fig3SA1A2B1B2.jpg](#)
- [supplement1POS.xls](#)

- QCnegTIC.png
- supplement2D1vsD8.xls
- supplement1NEG.xls
- supplement3D1vsD15..xls
- supplement3D1vsD15..xls
- supplement2NEGD1vsD8.xls
- supplement1POS.xls
- Fig2SA1A2B1B2.jpg
- Fig4SA1A2B1B2.jpg
- supplement5NEGD1vsS29.xls
- supplement5NEGD1vsS29.xls
- supplement4D1vsD15..xls
- Fig3SA1A2B1B2.jpg
- supplement2NEGD1vsD8.xls
- QCnegTIC.png
- supplement2D1vsD8.xls
- supplement1NEG.xls
- QCposTIC.png
- supplement5posD1vsD29.xls